

# Stimulated Brillouin scattering with distributed feedback

O. P. Zaskal'ko, A. A. Zozulya, Yu. I. Kyzylasov, N. B. Panaioti, V. P. Silin, V. T. Tikhonchuk, and I. L. Fabelinskii

*P. N. Lebedev Physical Institute, Academy of Sciences USSR*

(Submitted 8 May 1984)

Zh. Eksp. Teor. Fiz. **87**, 1582–1593 (November 1984)

Low-threshold stimulated Mandel'shtam-Brillouin (SMBS) scattering with distributed feedback is realized in carbon bisulfide. The effect is due to Bragg diffraction of the SMBS radiation by the space-periodic lattice of the refractive index, induced in the optically nonlinear medium as a result of interference of the exciting-light beams incident on and reflected by the mirror. Single-frequency SMBS radiation generation, with a low angular divergence and high energy efficiency, is attained. A theory is developed that can be employed to calculate the nonlinear coefficient of pump conversion into SMBS radiation and to determine the optimal generation direction. Good agreement is observed between the theory and experiment.

## 1. INTRODUCTION

Stimulated Mandel'shtam-Brillouin scattering (SMBS) arises as the result of nonlinear interaction of intense stimulating light with a material medium.<sup>1</sup> It corresponds to the process of decay of the exciting light wave into another scattered light wave and a hypersound wave. Under the assumption of a specified intensity of the exciting light, the intensity of the scattered radiation increases exponentially in space (convective instability). Significant intensity of the scattered radiation can be achieved under such conditions only for very high values of the coefficient of exponential amplification  $\sim 20$ – $30$ .

The SMBS threshold can be lowered significantly if positive feedback can be created in the SMBS excitation. Here, an exponential growth of the intensity of the scattered radiation in time takes place (absolute instability<sup>2</sup>). As a rule, this is achieved by excitation of SMBS in an optical resonator of the type of a Fabry-Perot interferometer, where the so-called "lumped feedback" takes place—the interaction of the oncoming waves is produced in fixed cross sections of space. The necessary condition for high energy efficiency of the SMBS is saturation of the gain. In the resonator, it can be accompanied by a cascade generation of the SMBS components,<sup>3</sup> significantly degrading the monochromatic character of the generated radiation.

A regime of absolute instability can also develop in the cavity-free excitation of scattering, for example, when the SMBS is excited by two antiparallel light beams.<sup>4–6</sup> In this latter case, absolute instability arises in the case of SMBS only from the simultaneous excitation of the Stokes and anti-Stokes components of the scattered field. For this reason, the threshold of such parametric generation is not much lower than the threshold of the ordinary convective SMBS. Much lower thresholds of generation exist in this case if the parametric coupling can be realized without participation of the anti-Stokes components.<sup>7</sup>

In the present work, low-threshold SMBS with distributed feedback is proposed for the first time and then experimentally realized for the case of almost antiparallel pump beams, and a theory of this phenomenon is developed.

Distributed feedback exists because of the Bragg diffraction of the SMBS radiation by the spatially periodic lattice of the index of refraction, induced in an optically nonlinear medium as a result of the interference of two light beams.

Since the distributed feedback possesses a much higher spectral selectivity in comparison with the "lumped back",<sup>8</sup> the SMBS excitation used in such a scheme allows us to obtain single-frequency generation, which possesses a high energy efficiency and low angular divergence. The theory developed here for this phenomenon permits us to calculate the coefficient of transformation of the pump energy into the SMBS radiation, and to determine the optimal direction of the generation and distribution of the amplitudes of the waves interacting in the nonlinear medium. A comparison of the experimental results with the theoretical results shows excellent agreement between the two.

## 2. SETUP OF THE EXPERIMENT AND EXPERIMENTAL RESULTS

The experimental setup is depicted in Fig. 1. On a cell filled with carbon disulfide, with internal dimension  $l_0 = 6$

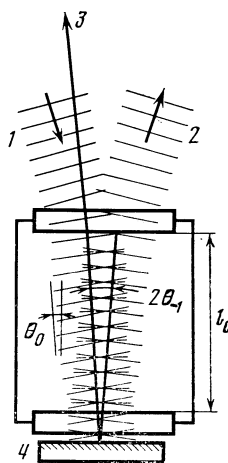


FIG. 1. Experimental setup: 1—incident light beam, 2—reflected light beam, 3—direction of SMBS generation, 4—mirror.

cm, a collimated light beam of circular cross section was incident obliquely in the direction 1. The beam was generated by a single-frequency, single-mode neodymium laser (wavelength  $\lambda_0 = 1.06 \mu$ ). The beam was collimated by a mirror with radius of curvature 2 m in such fashion that its diameter in the cell amounted to  $d = 1$  mm. Passing through the cell, the laser beam was reflected almost directly backward in the direction 2 by the plane mirror 4 with reflection coefficient 0.99. This mirror was located in back of the rear window of the cell. The minimum distance between the boundaries of the liquid and the mirror was limited by the thickness of the windows of the cell, and amounted to 0.8 cm. Reflection from the window of the cell amounted to 0.04. To prevent the appearance of parasitic resonators in the process of excitation of the SMBS, the cell was mounted in such fashion that the planes of its windows were not parallel to the plane of the mirror 4.

The mechanism of formation of distributed feedback can be illustrated qualitatively as follows. The incident (1) and reflected (2) laser beams interfere with one another in the region of overlap. As a consequence of the dependence of the index of refraction of the medium on the intensity of the light wave  $n_E = n(1 + 1/2n_2|E|^2)$  a three-dimensional phase grating of the index of refraction develops in the medium, with a period  $\sim \lambda_0/2n \cos \theta_0$ , where  $2\theta_0$  is the angle between the incident and reflected beams of the laser in the medium (see Fig. 1). The radiation arising as a result of the SMBS of the incident and reflected light beams, with wavelength  $\lambda_{-1} = \lambda_0(1 + 2nv_s/c)$ , where  $v_s$  is the sound velocity in the medium and  $c$  is the light velocity in vacuum, is diffracted by this grating. The Bragg condition  $\cos \theta_{-1} = (\lambda_0/\lambda_{-1}) \cos \theta_0$  allows an approximate estimate of the angle  $\theta_{-1}$  between the direction of propagation of the SMBS radiation and the normal to the mirror 4 at which the distributed feedback arises. A more accurate relation between the angles  $\theta_{-1}$  and  $\theta_0$ , which takes into account the nonlinear phase shift of the interacting waves and the boundedness of the region of interaction, is given by Eq. (14) (see below).

Liquid carbon disulfide was used in the research as the optically nonlinear medium that is active in SMBS, as has already been noted. Such a choice was made because of the fact that carbon disulfide has the highest nonlinear index of refraction  $n_2 \approx 1.0 \cdot 10^{-11} \text{ cm}^3/\text{erg}$  (Ref. 9) of all simple liquids, and also the largest value of the increment of SMBS, equal to  $4 \cdot 10^{-2} \text{ cm/MW}$  at a wavelength of the exciting light  $\lambda_0 = 1.06 \mu$ .<sup>10</sup> The index of refraction and the sound velocity of carbon bisulfide are respectively equal to  $n = 1.61$  and  $v_s = 1.2 \cdot 10^5 \text{ m/s}$ .

The spectral, temporal and energy parameters of the SMBS radiation and of beams 1 and 2 of the exciting radiation were studied experimentally. The divergence of the radiation and the dependence of the direction of generation of the SMBS on the angle between beams 1 and 2 were also studied. The energy of the radiation was measured by a calorimeter of the type IKT-1N. The time analysis of the dynamics of the radiation was carried out with coaxial photocells of the type FÉK-15 and FÉK-09, connected to a high speed oscilloscope S7-10b and to the storage oscilloscope S8-12. The triggering for scanning of the oscilloscopes was

brought about by means of additional photocells of the laser radiation; the instability of the triggering amounted to less than 5 ns. The spectral analysis of the radiation was accomplished with a Fabry-Perot interferometer with a free spectral range  $1 \text{ cm}^{-1}$  after preliminary doubling of the frequency of the radiation in a  $\text{LiIO}_3$  crystal.

Two series of experiments were carried out in the case of energy and duration  $\tau$  of the exciting laser pulse of 21 mJ, 40 ns and 19 mJ, 60 ns, respectively. In the first series ( $\tau = 40$  ns), the effective generation of SMBS was observed under conditions in which the angle  $\theta_0$  was varied in the range from 3.4 mrad to 5.4 mrad. The SMBS was generated in the plane of incidence of the wave of exciting light; then the beam of SMBS radiation 3 (Fig. 1) was deflected from the normal to the mirror 4 in the direction of the wave entering into the cell. The angle  $\theta_{-1}$  between the direction of propagation of the SMBS radiation in the cell and the direction of the normal to the mirror 5 amounted to 0.6 mrad at  $\theta_0 = 3.4$  mrad and 1.5 mrad at  $\theta_0 = 5.4$  mrad. The SMBS radiation was a well-collimated beam of circular cross section with a divergence of not more than 0.5 mrad, approximately twice the divergence of the exciting light. At an exciting pulse energy kJ incident on the cell with the carbon disulfide, the energy of the radiation emerging from the cell was distributed as follows: 6 mJ of SMBS radiation in the direction 4; 8 mJ specularly reflected in the direction 2; the remaining 6 mJ of the exciting pulse was lost to parasitic reflection from the cell windows (4 mJ) and to absorption in the carbon disulfide. The energy efficiency of the SMBS was 30%.

The dynamics of generation of SMBS with distributed feedback are shown in Fig. 2b. For comparison, the oscillograms of radiation incident on the cell with the carbon disulfide in the direction 1, and emerging from it in the direction 2, are shown in Figs. 2a and c. These were obtained in the same scale and at the same stage of triggering of the recording system as the oscillogram in Fig. 2b. It follows from the given oscillograms that the intense generation of SMBS (Fig. 2b) begins within about 20 ns after the beginning of the exciting pulse (Fig. 2a). The front of the SMBS pulse is steeper than the front of the exciting pulse. The generation of SMBS is accompanied by the depletion of the exciting wave emerging from the cell in the direction 2 (Fig. 2c). At maximum

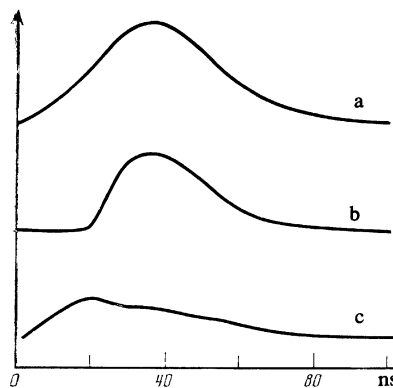


FIG. 2. Oscillograms of the incoming pump wave (a), the exciting SMBS radiation (b) and the radiation of the pump exciting in the specular direction (c). The scales of the oscillograms are the same.

SMBS generation, the power of the SMBS radiation amounted to more than 80% of the maximum power of the incident pulse 1 (Fig. 2a) and almost three times the maximum power of the reflected wave 2 (Fig. 2c). Thus the observed SMBS generation was accompanied by a strong saturation of the gain and depletion of the pump.

The results of spectral measurements of the radiation emerging from the cell are shown in Fig. 3. An interferogram of the radiation at double frequency, emerging in the direction 3 (the inner set of rings) is shown in Fig. 3a, along with an interferogram of the second harmonic of the laser beam (the outer set of rings). It is seen that only a single spectral component of the second harmonic radiation in the direction 3 is present in the spectrum, shifted in the Stokes direction by  $0.25 \text{ cm}^{-1}$ . The accompanying spectral shift at the basic frequency ( $0.125 \text{ cm}^{-1}$ ) corresponds to a shift in the SMBS line in carbon disulfide in the backward direction. In the spectrum of radiation reflected in direction 2, there is only a single spectral line of the laser (Fig. 3b). It should be noted here that the SMBS radiation contains only the first Stokes component, in spite of the fact that the SMBS process, as has been noted above, takes place under conditions of saturation of the amplification.

In the second set of experiments ( $\tau = 60 \text{ ns}$ ) effective SMBS generation was observed in the range of angles  $3.2 < \theta_0 < 5.0 \text{ mrad}$ . The corresponding values of the angle  $\theta_{-1}$  between the direction of SMBS generation and the normal to the mirror 4 are shown in Fig. 4. As is seen from this drawing, the dependence of the value of the angle  $\theta_{-1}$  on the values of the angle  $\theta_0$  is nonmonotonic. It has been possible to excite the SMBS generation effectively at  $\theta_0 = 1.3 \text{ mrad}$ . Here the angle  $\theta_{-1}$  amounted to at most 0.3 mrad. For the angles of incidence of the laser radiation specified above, the amplitude of the pulse of SMBS radiation reached 50–60%, while the beginning of the generation was delayed relative to the beginning of arrival of the pump pulse at the cell by 50 ns. The shapes of the pulse of the exciting radiation and of the SMBS radiation were similar to those shown in Figs. 2a and b. Upon increase in the angle  $\theta_0 > 5 \text{ mrad}$ , the amplitude coefficient of SMBS conversion decreased sharply and at  $\theta_0 > 8 \text{ mrad}$  it amounted to  $4 \cdot 10^{-3}$ . Here the SMBS was excited strictly in the back direction.

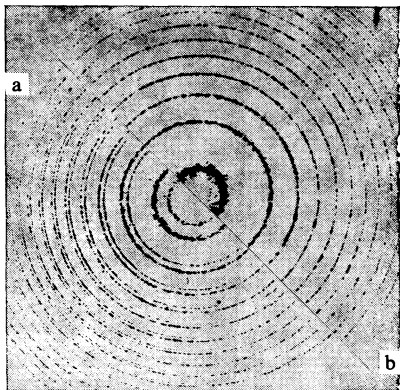


FIG. 3. a) Interferograms of the SMBS radiation (inner system of rings) and of the pump radiation (outer system of rings) b) Interferogram of the radiation specularly reflected in the direction 2 in Fig. 1.

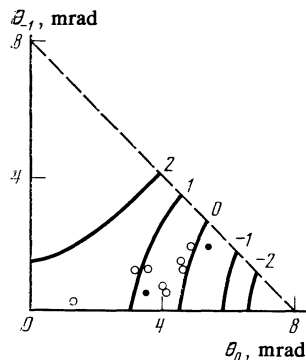


FIG. 4. Dependence of the threshold direction of the SMBS generation  $\theta_{-1}$  on the angle of the incidence  $\theta_0$  of the pump radiation at  $\Delta = 0$ . The numbers of the curves correspond to the numbers of the excited modes. The calculation is carried out according to Eq. (11) for the conditions of experiment:  $r^2 = 0.9$ ;  $n_2/G = 0.3$ ;  $l_0 = 6 \text{ cm}$ ;  $d = 1 \text{ mm}$ ; the dashed line is the boundary of the strong overlap of the beams, the points are measurements in the first (●) and second (○) set of experiments.

### 3. THEORY

In this section, we shall set forth the nonlinear theory of SMBS with distributed feedback, which will then be used for the analysis of the experimental results. The distributed feedback considered here is due to the mutual diffraction of scattered Stokes waves by the refractive-index grating created by the exciting waves incident on and reflected by the mirror. This process is one of the possible manifestations of coherent SMBS excited in the medium by the incident and reflected waves, called in Ref. 7 double stimulated Mandelstam-Brillouin scattering (DSMBS).

We consider a one-dimensional model, assuming the fronts of the interacting waves to be plane. Let a wave of frequency  $\omega_0$  be incident from above on a layer of nonlinear medium of thickness  $l$  ( $0 < x < l$ ). The lower boundary ( $x = l$ ) specularly reflects the waves incident on it with an amplitude reflection coefficient  $re^{i\psi}$ . Consequently, two exciting waves are present in the medium—the incident  $E_{01}$  and the reflected  $E_{0-1}$ .

In correspondence with the general premises of DSMBS theory that the excitation of absolute instabilities have a high threshold connected with the presence of anti-Stokes components,<sup>7</sup> and in accordance with experiment, we shall assume that only the Stokes components of the scattered light  $E_{-1\sigma}$  ( $\sigma = \pm 1$ ) are excited. Therefore, the optical electric field in the medium has the form

$$E_z(\mathbf{r}, t) = \text{Re}[E(x, y, t) e^{-i\omega_0 t}], \quad (1)$$

where

$$E(x, y, t) = \sum_{\sigma=\pm 1} [E_{0\sigma}(x) \exp(i\sigma k_{0x}x + ik_{0y}y) + E_{-1\sigma}(x) \times \exp(i\sigma k_{-1x}x + ik_{-1y}y + i\Omega t)]. \quad (2)$$

Here  $k_{0x} = k_0 \cos \theta_0$ ,  $k_0 = n\omega_0/c = (k_{0x}^2 + k_{0y}^2)^{1/2}$ ,  $k_{-1x} = k_{-1} \cos \theta_{-1}$ ,  $k_{-1} = n(\omega_0 - \Omega)/c$ . The amplitudes of the light field obey the boundary conditions imposed on the field on the upper edge of the layer  $E_{01}(0) = E_0$ ,  $E_{-11}(0) = 0$  and the conditions of specular reflection of the waves from the lower edge

$$E_{0,-1}(l) = r e^{i\psi} E_{01}(l), \quad E_{-1,-1}(l) = r E_{-11}(l) e^{i\psi - 2iq l},$$

where  $q = k_{0x} - k_{-1x}$ . Such a statement of the problem is typical for DSMBS theory (see Ref. 7).

In the nonlinear equations written for the field, we take into account two mechanisms of nonlinearity. First there is the mechanism of orientation nonlinearity, which leads to a change in the dielectric constant  $\delta\epsilon_K = n^2 n_2 |E|^2 > 0$ . Then we take into consideration the SMBS stricture change in the dielectric constant which determines the ordinary and is due to the field beats at the frequency of the sound wave

$$\delta\epsilon_s = \frac{ik_s Y^2}{32\pi\rho v_s^2 \alpha (1-i\Delta)} \times \sum_{\sigma=\pm 1} E_{0\sigma} E_{-1-\sigma} \exp(i\sigma k_{sx} x + ik_{sy} y - i\Omega t) + \text{c.c.}, \quad (3)$$

where  $Y = \rho \partial \epsilon / \partial \rho$  is the parameter of stricture nonlinearity,  $\rho$ , is the density of the medium,  $k_{sx} = k_{0x} + k_{-1x}$ ,  $k_{sy} = k_{0y} + k_{-1y}$ ,  $\Delta = (\Omega / v_s - k_s) / \alpha$  is the departure of the frequency of the sound from its resonance value,  $\alpha$  is the amplitude coefficient of sound absorption. Corresponding to such mechanisms of nonlinearity, we can limit ourselves to the following truncated equations:

$$\begin{aligned} \sigma \frac{dE_{0\sigma}}{dx} &= \frac{k_0^2}{2k_{0x}} \left\{ -\frac{G}{1-i\Delta} E_{0\sigma} |E_{-1-\sigma}|^2 + in_2 E_{0\sigma} \right. \\ &\quad \times \left[ 2 \sum_{\sigma'=\pm 1} (|E_{0\sigma'}|^2 + |E_{-1\sigma'}|^2) \right. \\ &\quad \left. \left. - |E_{0\sigma}|^2 \right] + 2in_2 E_{0-\sigma} E_{-1\sigma} E_{-1-\sigma} \exp(-2i\sigma q x) \right\}, \\ \sigma \frac{dE_{-1\sigma}}{dx} &= \frac{k_0^2}{2k_{0x}} \left\{ \frac{G}{1+i\Delta} E_{-1\sigma} |E_{0\sigma}|^2 + in_2 E_{-1\sigma} \right. \\ &\quad \times \left[ 2 \sum_{\sigma'=\pm 1} (|E_{0\sigma'}|^2 + |E_{-1\sigma'}|^2) \right. \\ &\quad \left. \left. - |E_{-1\sigma}|^2 \right] + 2in_2 E_{0\sigma} E_{0-\sigma} E_{-1-\sigma} \exp(2i\sigma q x) \right\}, \end{aligned} \quad (4)$$

where  $G = (k_s Y^2 / 32\pi a n^2 \rho v_s^2)$ . Here, since  $|q| \ll k_0$ , the difference between  $k_{0x}$  and  $k_{-1x}$  is taken into account in Eq. (4) only in the exponentials. The right sides of Eqs. (4) describe three nonlinear, spatially distributed optical processes: first, the convective amplification of the Stokes components and the weakening (depletion) of the exciting light, which corresponds to ordinary SMBS; second, the nonlinear change in the index of refraction, and third, the distributed feedback that is necessary for the SMBS, and that is due to the mutual diffraction of the pair of exciting waves by the refractive-index grating created by the Stokes waves, as well as the pair of Stokes waves by the refractive-index grating due to the pair of exciting waves.

Under conditions of the smallness of the ratio  $n_2/G$  there is the possibility of constructing an approximate nonlinear solution of the system (4), using a small parameter ( $n_2/G \ll 1$ ). Since very few nonlinear solutions have been obtained

up to the present in SMBS theory, we shall describe our solution in some detail. First, we note that, upon neglect of  $n_2$ , Eqs. (4) describe two independent processes, while, by virtue of the boundary conditions,  $E_{-11} = 0$  in this approximation. Account of the small quantity  $n_2$  leads to the result that the amplitude  $E_{-11}$  turns out to be smaller by a factor of  $G/n_2$  than the other amplitudes. Basing ourselves on this fact and introducing the dimensionless amplitude of the waves ( $\mu = 0, -1$ )

$$e_{\mu\sigma} = \frac{E_{\mu\sigma}}{E_0} \exp \left[ -i\sigma \frac{n_2 k_0^2}{k_{0x}} \int_0^x dx' \sum_{\sigma'=\pm 1} (|E_{0\sigma'}|^2 + |E_{-1\sigma'}|^2) \right],$$

we find from the truncated equations (4), with accuracy to terms that are linear in  $n_2/G$ , the following set of equations:

$$\begin{aligned} \frac{de_{01}}{dx} &= \frac{1}{2} e_{01} \left( -\frac{g}{1-i\Delta} |e_{-1-1}|^2 - ih |e_{01}|^2 \right), \\ \frac{de_{0-1}}{dx} &= \frac{i}{2} h e_{0-1} |e_{0-1}|^2, \\ \frac{de_{-1-1}}{dx} &= \frac{1}{2} e_{-1-1} \left( -\frac{g}{1+i\Delta} |e_{01}|^2 + ih |e_{-1-1}|^2 \right), \\ \frac{de_{-11}}{dx} &= \frac{1}{2} \frac{g}{1+i\Delta} e_{-11} |e_{0-1}|^2 + ih e_{01} e_{0-1} e_{-1-1} e^{2iqx}, \end{aligned} \quad (5)$$

where  $g(k_0^2/k_{0x})G|E_0|^2$ ,  $h = (k_0^2/k_{0x})n_2|E_0|^2$ . Only the last equation of the set (4) contains the effect of the Bragg diffraction that transforms the wave  $e_{-1-1}$  into the wave  $e_{-11}$  on the refractive index grating that is produced by the incident and reflected components of the exciting light. Therefore, only this equation describes the effect of the distributed feedback.<sup>8</sup>

Using the notation  $R_0 = e_{0-1}(0)$ ,  $R_{-1} = e_{-1-1}(0)$  for the coefficients of reflection from the nonlinear layer at the frequencies  $\omega_0$  and  $\omega_0 - \Omega$  respectively, we can write down the following solutions of the first three equations of the system (5), which satisfy the boundary conditions on the upper boundary of the layer:

$$\begin{aligned} e_{01}(x) &= (1 - |R_{-1}|^2)^{1/2} \left[ 1 - |R_{-1}|^2 \exp \left( -gx \frac{1 - |R_{-1}|^2}{1 + \Delta^2} \right) \right]^{-1/2} \\ &\quad \times \exp \left\{ i \left[ -\frac{1}{2} hx (1 - |R_{-1}|^2) \right. \right. \\ &\quad \left. \left. + \frac{1}{2} \left( \Delta + \frac{h}{g} (1 + \Delta^2) \right) \ln |e_{01}|^2 \right] \right\}, \end{aligned} \quad (6)$$

$$\begin{aligned} e_{0-1}(x) &= R_0 \exp \left( \frac{i}{2} hx |R_0|^2 \right), \\ e_{-1-1}(x) &= R_{-1} \left( 1 - \frac{1 - |e_{01}|^2}{|R_{-1}|^2} \right)^{1/2} \exp \left[ \frac{i}{2} gx \Delta \frac{1 - |R_{-1}|^2}{1 + \Delta^2} \right. \\ &\quad \left. - \frac{i}{2} \left( \Delta + \frac{h}{g} (1 + \Delta^2) \right) \ln |e_{01}|^2 \right]. \end{aligned}$$

Graphs of the  $x$  dependence of the amplitude moduli are shown in Fig. 5. The monotonic falloff of amplitude of the exciting light with increase in  $x$  is accompanied by a growth (with decrease in the  $x$  coordinate) of the amplitude of the reflected Stokes component  $|e_{-1-1}|$ .

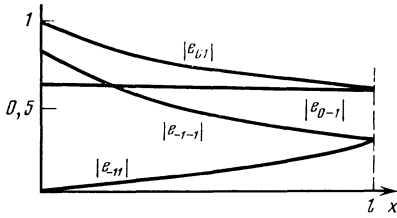


FIG. 5. Distribution of the moduli of the amplitudes of the pump waves and the scattered waves over the thickness of the layer. The coefficient of reflection of the mirror  $r=1$ , the coefficient of SMBS conversion  $|R_{-1}|^2=0.7$ , the ratio of the nonlinear susceptibilities  $G/n_2=5$ , fundamental scattering mode.

The boundary condition for the component of the exciting light wave on the lower boundary of the layer gives the connection between the reflection coefficients  $R_0$  and  $R_{-1}$ :

$$R_0 = r \left( \frac{1 - |R_{-1}|^2}{M} \right)^{1/2} \exp \left[ i\psi + \frac{3}{2} i h l (|R_0|^2 + 1 - |R_{-1}|^2) + i \left( \Delta - 7 \frac{h}{g} (1 + \Delta^2) \right) \ln \frac{|R_0|}{r} \right], \quad (7)$$

where  $M = 1 - |R_{-1}|^2 \exp[-gl(1 - |R_{-1}|^2)/(1 + \Delta^2)]$ . Equations (6) and (7) allow us to write down the solution of the last equation of the set (7) in explicit form for the field of the Stokes component traveling into the depth of the layer:

$$e_{-11}(x) = i h R_0 R_{-1} (1 - |R_{-1}|^2) \times \int_0^x dx' \left\{ 1 - |R_{-1}|^2 \exp \left( -g x' \frac{1 - |R_{-1}|^2}{1 + \Delta^2} \right) \right\}^{-1} \times \exp \left[ \frac{1}{2} \frac{g}{1 + i\Delta} |R_0|^2 (x - x') + 2i q x' - \frac{i}{2} h x' (|R_0|^2 + 1 - |R_{-1}|^2) - \frac{1}{2} g x' \frac{1 - |R_{-1}|^2}{1 + \Delta^2} \right]. \quad (8)$$

The amplitude  $e_{-11}$  can undergo oscillations, depending on the value of the phase of the integrand in Eq. (8). We shall call the number of maxima  $N$  of the function  $|e_{-11}|$  on the segment  $(0, l)$  the number of modes of the nonlinear state. The amplitude distribution in the layer for  $N=0$  is shown in Fig. 5.

Finally, using the boundary condition at  $x=l$  for the field of the Stokes component, we obtain the following relation, which determines the reflection coefficient  $|R_{-1}|$ :

$$1 = i r^2 \frac{h}{g} \int_0^l \frac{dv}{1 - |R_{-1}|^2 \exp(-v/(1 + \Delta^2))} \exp \left[ \frac{1}{2} \left( 1 + \frac{r^2}{M^2} \right) \times (v - v_0) \left( \frac{1}{1 + i\Delta} + i \frac{h}{g} - \frac{4iq}{g(1 - |R_{-1}|^2)(1 + r^2/M^2)} \right) \right], \quad (9)$$

where  $v_0 = gl(1 - |R_{-1}|^2)$ .

For an understanding of the conditions of applicability of the approximate system (5) and the solution obtained from

it, we must note that it does not take into account the effect of depletion of the reflected component of the exciting light wave  $e_{0-1}$ . Because of the smallness of the amplitude of the wave  $|e_{-11}| \sim h/g$ , the effect of depletion of the wave  $e_{0-1}$  not taken into account in (5) becomes important at  $h^2 l > g$ . Therefore, the use of the system (5) and its consequences is possible for not very high intensities of the exciting wave, namely, when

$$gl < (G/n_2)^2. \quad (10)$$

For the subsequent comparison of theory and experiment, it is necessary to consider the consequences of Eq. (9). First of all, setting  $R_{-1} = 0$  in (9), we obtain the following complex equation for the boundary of absolute instability—the generation of DSMBS:

$$gla = -i\pi \left( 2N + \frac{1}{2} \right) + \ln \left( i + \frac{ga}{r^2 h} \right), \quad a = \frac{1+r^2}{2} \left( \frac{1}{1+i\Delta} + i \frac{h}{g} - \frac{4iq}{g(1+r^2)} \right), \quad (11)$$

where  $N$  is an integer. Here, if  $2\pi N < \ln(G/n_2 r^2)$ , then the limiting value of  $g$  does not depend on  $N$  (compare with Ref. 8) and the real part of the complex equation (11) gives

$$gl = 2 \frac{1 + \Delta^2}{1 + r^2} \ln \left[ \frac{(1+r^2)g}{2r^2 h (1 + \Delta^2)} \right]. \quad (12)$$

In accord with this, the minimum threshold of absolute instability corresponds to  $\Delta = 0$ , i.e., to resonance excitation of the sound wave ( $\Omega = k_s v_s$ ).

Modes with different numbers correspond to generation of waves at different angles. Thus, at small  $N$ , in accord with the imaginary part of Eq. (11), we have

$$(k_{0x} - k_{-1x})l = \frac{\pi}{4} - \pi N + \frac{1+r^2}{4} l \left( h - \frac{g\Delta}{1 + \Delta^2} \right), \quad (13)$$

which differs from the simple condition of Bragg synchronism  $k_{0x} = k_{-1x}$ . The fact that  $ql \gg 1$  on the threshold of SMBS generation makes it possible to detail the consequences of Eq. (9) even above the threshold of absolute instability. Thus, for the small angles  $\theta_0 \ll 1$  used in experiment, and for the fundamental mode  $N=0$ , the direction of generation is, in accord with (13), given by the formula

$$\theta_{-1} = \left[ \theta_0^2 - 4n \frac{v_s}{c} + \frac{\lambda_0}{4nl} + \frac{\lambda_0}{4n\pi} (1+r^2) (1 - |R_{-1}|^2) \left( h - \frac{g\Delta}{1 + \Delta^2} \right) \right]^{1/2} \quad (14)$$

which characterizes the difference of such a direction from the usual value  $(\theta_0^2 - 4nv_s/c)^{1/2}$ , which is obtained from the conditions of coherent Bragg scattering by the lattice of the field of the exciting light. In addition, it turns out to be possible to write down the following equation for the conversion coefficient  $|R_{-1}|^2$ :

$$1 - |R_{-1}|^2 = \frac{2(1 + \Delta^2)}{gl(1 + r^2)} \ln \left[ \frac{GF(r^2, |R_{-1}|^2)}{n_2 r^2 (1 + \Delta^2)} \right], \quad (15)$$

here

$$F(r^2, |R_{-1}|^2) = \left[ \int_0^1 ds (1-s|R_{-1}|^2)^{-1} s^{-(1-r^2)/2} \right]^{-1}.$$

At the same time

$$F(1, |R_{-1}|^2) = -|R_{-1}|^2 \ln^{-1}(1-|R_{-1}|^2);$$

$$F(0, |R_{-1}|^2) = \ln^{-1}[(1+|R_{-1}|)/(1-|R_{-1}|)].$$

Furthermore, in the case  $|R_{-1}|^2 \ll 1$ , we have  $F(r^2, |R_{-1}|^2) \approx (1+r^2)/2$ , while at  $1-|R_{-1}|^2 \ll 1$  we have  $F(r^2, |R_{-1}|^2) \approx -\ln^{-1}(1-|R_{-1}|^2)$ . It follows from Eq. (15) that  $|R_{-1}|^2$  increases monotonically upon increase in the intensity of the exciting wave. The graph of the dependence of the reflection coefficient of the Stokes component  $|R_{-1}|^2$  on  $gl$  at  $\Delta = 0$  is shown in Fig. 6. It is seen that at twice the threshold level, 50 per cent transformation of the exciting signal into the Stokes component is achieved. Moreover, the possibility is seen of almost complete transformation without violation of condition (10).

We now consider the dependence of the intensity of the Stokes component on the detuning. According to (15), the maximum value of  $|R_{-1}|$  is achieved at  $\Delta = 0$ . Along with this, the possibility of generation of the Stokes components with large detuning  $|\Delta| < \Delta_{\max} \sim (gl)^{1/2}$  is seen from this same formula. Therefore, our theory predicts the possibility of a sufficiently wide spread of frequencies of the Stokes component with  $\delta\omega \sim av_s(gl)^{1/2}$ .

In conclusion, we pause to consider the single DSMBS regime that was treated in Ref. 7, and that is due only to the stricture nonlinearity and leads to the change from specular reflection to backward reflection of the Stokes component. In such a regime, the time of development of an absolute instability is determined by the damping time of the sound waves propagating perpendicular to the  $x$  axis with frequency  $2k_{0y}v_s$ . Since  $k_{0y} \ll k_{0x}$  under the experimental conditions, the damping time of such waves exceeds the duration of the pulse by more than an order of magnitude and no absolute instability can develop. In contrast, the damping time of sound waves, given by the truncated equations (4) and (5), is significantly less than the pulse duration. This, together with the practically inertia-free orientation nonlinearity, guarantees the possibility of realization of the absolute instability of DSMBS considered theoretically here, under the experimental conditions set forth above.

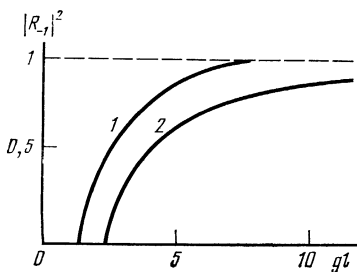


FIG. 6. Dependence of the SMBS conversion coefficient  $|R_{-1}|^2$  on the coefficient of convective amplification of the SMBS  $gl$  for the case  $n_2/G = 0.3$ ,  $r^2 = 0.9$ —curve 1 and  $n_2/G = 0.1$ ,  $r = 1$ —curve 2, fundamental mode of scattering.

#### 4. DISCUSSION OF RESULTS

In the comparison of the predictions of theory with experiment it is necessary to take into account the boundedness of the region of overlap of the beams. It is seen from Fig. 1 that the vertical cross section of the region of overlap of the incident and reflected light beams in the plane of the drawing is a triangle of height  $d/2\theta_0$ . Therefore, the depth of the cell  $l_0$  can be taken as the interaction length only for small angles  $\theta_0 \lesssim d/2l_0 \approx 8$  mrad and only for small angles of propagation of the SMBS radiation  $\theta_{-1} + \theta_0 \lesssim d/2l_0$ .

For large angles  $\theta_{-1}$  we must expect a sharp increase in the generation threshold because of the shortening of the path length of the beam of SMBS in the region of overlap of the beams.

Further, the reflection coefficient of the mirror 4 (Fig. 1) amounts to 99, but on the glass—air interface there is an additional reflection at each passage of the beams. Therefore, the reflection coefficient must be taken to be  $r^2 = 0.9$ .

According to the parameter of nonlinearity for carbon disulfide given in Sec. 2,

$$(8\pi n/c) k_0 G = g/I = 4 \cdot 10^{-2} \text{ cm/W},$$

$$(8\pi n/c) k_0 n_2 = h/I = 1.25 \cdot 10^{-2} \text{ cm/W},$$

where  $I$  is the intensity of the entering light beam 1 (Fig. 1). Hence, the ratio of the parameters or orientation and stricture nonlinearity for carbon disulfide is given by  $h/g \approx 0.3$ .

Calculation of the generation thresholds of SMBS from Eq. (11) for the parameters given above at  $\Delta = 0$  gives the results shown in the table for the first five modes.

The corresponding dependences of the threshold directions of generation of  $\theta_{-1}$  from  $\theta_0$  are shown in Fig. 4. The region in which the one-dimensional theory of SMBS generation is applicable is bounded by the dashed line. In correspondence with the table and Fig. 4, we can state that the SMBS with the lowest threshold at the mode  $N = 0$  is possible at angles  $4.5 < \theta_0 < 5.5$  mrad. At large angles of incidence of the pump, generation at the modes  $N = -1$  and  $N = -2$  is possible. In the range of angles  $3.5 < \theta_0 < 5.3$  mrad, where SMBS generation was observed in the first series of experiments, minimal thresholds were achieved for the modes  $N = 0$ , and 1. Apparently, these are the modes in which generation took place. The experimentally measured values of the generation angle, shown in Fig. 4 by points, also confirm this.

In the first series, the experiments were carried out at a power of 0.52 MW at the maximum of the pulse; in the case

TABLE I. Generation threshold of SMBS, values of the detuning of the wave numbers  $ql$  and limiting angle of generation  $\theta_0^*$  for the first five modes (the calculation is carried out according to Eq. (11) for the experimental conditions  $r^2 = 0.9$ ,  $n_2/G = 0.3$ ,  $l_0 = 6$  cm.

| $N$ | $g_{\text{thr}}, \text{cm}^{-1}$ | $ql$ | $\theta_0^*, \text{mrad}$ |
|-----|----------------------------------|------|---------------------------|
| 0   | 0,29                             | 1,5  | 4,5                       |
| -1  | 0,41                             | -2,9 | 5,9                       |
| 1   | 0,41                             | 4,9  | 3,0                       |
| -2  | 0,44                             | -5,7 | 6,6                       |
| 2   | 0,47                             | 8,2  | —                         |

of a beam diameter  $d = 1$  mm, this corresponds to an energy flux  $I_{\max} = 66$  MW/cm<sup>2</sup> and  $g_{\max} l_0 \approx 17$ ; in the second series, the power reached 0.3 MW, which corresponds to  $g_{\max} l_0 \approx 10$ . Thus, the excess over threshold at the maximum of the pulse reached 9 in the first series of experiments and 5 in the second. It then follows, in particular, that in the first series of experiments generation could be observed over a wider range of frequencies than was actually used in the experiment.

We now consider the dynamics of the generation.

The time growth rate of the absolute instability  $\gamma = \alpha v_s \operatorname{Im} \Delta$ , as follows from Eq. (11), is proportional to the damping decrement of the sound wave  $\gamma_s = \alpha v_s$ :

$$\gamma(t) = \gamma_s (g(t)/g_{\text{thr}} - 1). \quad (16)$$

In the linear stage, the intensity of the SMBS signal increases exponentially with time:

$$\propto \exp 2 \int_0^t \gamma(t) dt.$$

For an estimate of the value of the damping decrement, we use the formula for the SMBS gain  $G$  [see Eq. (4)]. Since the value  $g/I$  is known to us and all the remaining parameters of carbon disulfide are known ( $Y = 2.15$ ;  $\rho = 1.26$  g/cm<sup>3</sup>;  $v_s = 1.2 \cdot 10$  cm/s, we find from the expression for  $G$  that  $\alpha \approx 5 \cdot 10^3$  cm<sup>-1</sup>,  $\gamma_s \approx 6 \cdot 10^8$  s<sup>-1</sup>.

The ratio of the intensity of the spontaneous scattering of light in carbon disulfide into the solid angle of the recording system to the intensity of the pump for the conditions of our experiment amounts to  $\sim 10^{-10}$ . Therefore, if we start out from the fact that for the recording of SMBS generation, it is necessary that its intensity be  $\geq 1\%$  of the intensity of the pump, then we have the condition for the generation delay time  $t_0$

$$2\gamma_s \int_0^{t_0} dt (g(t)/g_{\text{thr}} - 1) \approx \ln 10^8 \approx 18.5.$$

Hence, for the first set of experiments, the delay time  $t_0 \approx 20$  ns, which is close to the experimental value (see Fig. 2). At the maximum of the laser pulse, the quantity  $2\int_0^{t_0} \gamma dt$  reaches the value  $\sim 100$  and consequently, a nonlinear state is realized that is close to stationary. Therefore, the experimentally measured conversion coefficient  $|R_{-1}|^2 \approx 80\%$  is close to the prediction of the nonlinear theory (for  $gl = 17$  we have from (15)  $|R_{-1}|^2 \approx 95\%$ ), while on the trailing edge of the laser pulse, the shape of the Stokes signal repeats the shape of the pump (see Fig. 2).

For the second set of experiments ( $\tau = 60$  ns), the calculated time of delay of generation amounts to 40 ns relative to the start of the pump pulse. This is also close to the experimental value  $\sim 50$  ns. The values of the conversion coefficient recorded in the second set of experiments reached  $\geq 50\%$ , which is somewhat less than the value  $\sim 80\%$  predicted by the theory. The somewhat smaller values of the measured conversion coefficients, in comparison with the

theoretically predicted values, are evidently connected with the fact that the assumption made in the nonlinear theory on the smallness of the ratio  $h/g$  carbon disulfide is quite inadequately satisfied, while the experimental realization of the value of  $gl$  lies outside the limits of the inequality (10).

There is good qualitative agreement with the theory in the investigations of the dependence of the direction and intensity of the generation on the angle of incidence of the pump wave as carried out in the second set of experiments. The nonmonotonic dependence  $\theta_1(\theta_0)$  at small angles  $\theta_0 < 7$  mrad corresponds to SMBS generation at different modes. The open circle in Fig. 4 show the values of  $\theta_{-1}$  measured in the second set.

At  $\theta_0 > 8$  mrad, the intensity of the SMBS radiation becomes a constant, independent of the angle  $\theta_0 \ll 1$ , corresponding to the usual convective SMBS backward. Knowing the level of spontaneous scattering and taking it into account that the amplification takes place both in the incident and the reflected pump waves, we can determine the value of  $(g_{\max} l_0)_{\text{exp}}$  achieved in our experiment. For  $|R_{-1}|^2 \approx 0.4\%$  at angles  $\theta_0 > 8$  mrad, we find  $(g_{\max} l_0)_{\text{exp}} \approx 9$ , which is excellent agreement with the calculated value  $g_{\max} l_0 \approx 10$ .

The good agreement of the theory and experiment allows us to confirm that SMBS due to distributed feedback by the refractive-index grating has been observed in the experiment.

The proposed scheme of SMBS converter is distinguished by its low generation threshold, high quantum yield, absence of higher Stokes components and small angular divergence of the radiation, which makes such a source promising.

<sup>1</sup>V. S. Starunov and I. L. Fabelinskii, Usp. Fiz. Nauk **98**, 441 (1969) [Sov. Phys. Uspekhi **11**, 463 (1970)].

<sup>2</sup>N. Kroll, J. Appl. Phys. **36**, 34 (1965).

<sup>3</sup>O. P. Zaskal'ko, Yu. N. Serdyuchenko, V. S. Starunov and I. L. Fabelinskii, Pis'ma Zh. Eksp. Teor. Fiz. **31**, 103(1980) [JETP Lett. **31**, 94 (1980)].

<sup>4</sup>B. Ya. Zel'dovich and V. V. Shkunov, Kvantovaya elektron. **9**, 393 (1982) [Sov. J. Quant. Electron. **12**, 223 (1982)].

<sup>5</sup>N. F. Andreev, V. P. Bespalov, A. M. Kiselev, G. A. Pasmanik, and A. A. Shilov, Zh. Eksp. Teor. Fiz. **82**, 1047 (1982) [Sov. Phys. JETP **55**, 612 (1982)]; V. I. Bespalov, E. L. Budis, S. N. Kulagina, V. F. Manishin, A. Z. Matveev, G. A. Pasmanik, R. S. Razenshtein and A. A. Shilov, Kvantovaya elektron. **9**, 2367 (1982) [Sov. J. Quantum Electron. **12**, 1544 (1982)].

<sup>6</sup>A. A. Zozulya, V. P. Silin and V. T. Tikhonchuk, Kratkie soobshcheniya po fizike (Short Communications in Physics) No. 10, 38 (1983).

<sup>7</sup>A. A. Zozulya, V. P. Silin and V. T. Tikhonchuk, Pis'ma Zh. Eksp. Teor. Fiz. **38**, 348 (1983) [JETP Lett. **38**, 52 (1983)]; Zh. Eksp. Teor. Fiz. **86**, 1296 (1984) [Sov. Phys. JETP **59**, 756 (1984)].

<sup>8</sup>H. Kogelnik and C. V. Shank, J. Appl. Phys. **43**, 2327 (1972).

<sup>9</sup>R. W. Hellwarth, J. Opt. Soc. Amer. **8**, 517 (1978).

<sup>10</sup>V. F. Efimkov, I. G. Zubarev, A. V. Kotov, A. B. Mironov and S. I. Mikhailov, Kvantovaya elektron. **8**, 891 (1981) [Sov. J. Quantum Electron. **11**, 533 (1981)].

Translated by R. T. Beyer